THE JOURNAL OF BIOLOGICAL CHEMISTRY VOL. 281, NO. 48, pp. 37215–37226, December 1, 2006

MAPK-activated Protein Kinase-2 (MK2)-mediated Formation and Phosphorylation-regulated Dissociation of the Signal Complex Consisting of p38, MK2, Akt, and Hsp27*

Received for publication, April 14, 2006, and in revised form, August 16, 2006 Published, JBC Papers in Press, October 2, 2006, DOI 10.1074/jbc.M603622200

Chunlei Zheng[‡], Ziyang Lin[§], Zhizhuang Joe Zhao[¶], Yajun Yang[‡], Hanben Niu[§], and Xun Shen[‡1]

From the [‡]Institute of Biophysics, and Graduate School, Chinese Academy of Sciences, 15 Datun Road, Choayang District, Beijing 100101, China, the [§]Institute of Optoelectronics, Key Laboratory of Opto-electronics Devices and Systems, Shenzhen University, Ministry of Education, Shenzhen 518060, China, and the [¶]Department of Pathology, University of Oklahoma Health Sciences Center, Oklahoma City, Oklahoma 73104

The p38 MAPK and heat shock protein 27 (hsp27) form a signaling complex with serine/threonine kinase Akt and MAPK-activated protein kinase-2 (MK2), which plays an important role in controlling stress-induced apoptosis and reorganizing actin cytoskeleton. However, regulation of the complex is poorly understood. In this study, the interaction between p38 and hsp27 was visualized in single living L929 cells using fluorescence resonance energy transfer technology, while their association with Akt was examined by immunoprecipitation analysis. Under normal growth conditions, p38 kinase constitutively interacts with hsp27. When cells were exposed to H_2O_2 or stimulated by arachidonic acid, this interaction was disrupted. However, inhibition of the activation of p38 and Akt by selective inhibitors or overexpression of the kinase-dead mutant of p38 diminished such effects. Furthermore, mutation of phosphorylation sites of hsp27 renders the interaction resistant to H_2O_2 and arachidonic acid. It was interesting to find that the interaction disappeared in the cells from MK2-knock-out mice or the cells treated with lemptomycin B that blocks export of MK2 from nucleus to cytosol. However, MK2 is not required for the association of hsp27 with Akt. This study suggests that MK2 mediates the incorporation of p38 into the pre-existing complex of hsp27 with Akt. Phosphorylation of hsp27 finally breaks the signaling complex.

The stress-activated p38 mitogen-activated protein kinase (MAPK)[2] and the stress-responsive heat shock protein 27 (hsp27) are two important proteins involved in cellular processes responding to extracellular stimuli and various stress (1–5). As a subgroup of the mammalian MAPKs, p38 has been found to be involved in inflammation, cell growth and differentiation, cell cycle, cell death (6), oxidative stress (4), and stimulation by cytokines such as tumor necrosis factor (5) and growth factors (7). Hsp27 usually exists as oligomers and plays a role in regulation of many cellular functions such as inhibition of the death receptor-mediated apoptosis (8), promotion of proper refolding of denatured proteins by acting as a molecular chaperone (9), and regulation of cytoskeleton (10). A large body of evidence has shown that hsp27 is a terminal substrate of the p38 MAPK cascade, and activation of p38 results in phosphorylation of Hsp27 that may change its intracellular distribution (11), modulate F-actin polymerization (12), and protect preconditioned hearts from sustained ischemia (13). Besides that, it has been well accepted that p38 MAPK is activated by dual phosphorylation on Thr and Tyr within a Thr-Gly-Tyr motif by MAPK kinases MKK3 and MKK6 (14, 15). Activated p38 phosphorylates MAPK-activated protein kinase-2 (MK2), which in turn phosphorylates heat shock protein 27 (16, 17). Thus, p38, MK2, and hsp27 are in a same signaling pathway.

Overwhelming evidence suggests that many signaling proteins form multimeric complexes held together by scaffolding proteins. Scaffolding proteins have been found for ERKs and JNKs, the two other members of the MAPK family (18, 19). Immunoprecipitation and glutathione *S*-transferase pull-down assays have demonstrated that the serine/threonine kinase Akt, p38, MK2, and hsp27 form a complex in neutrophils, and the activation of Akt results in dissociation of hsp27 from the complex upon neutrophil activation by *N*-formyl-methionyl-leucyl-phenylalanine. It has been suggested that this complex plays an important role in controlling stress-induced apoptosis (20, 21). The complex may provide a quick communication channel for hsp27 to implement its cellular functions in response to extracellular stimuli, such as protecting neuronal cells from heat shock and nerve growth factor withdrawal-induced apoptosis (22), reorganizing actin cytoskeleton under oxidative stress (23) or in the PDGF-induced lamellipodia formation and migration of the aortic smooth muscle cells (12), and modifying smooth muscle contraction (24). However, several questions remain for better understanding of this signaling complex. First, how is this complex formed? In other words, who is indispensable for the formation of the complex among these four signaling proteins? Second, it is unclear whether the dissociation of hsp27

* This work was supported by the National Natural Science Foundation of China (Grants 60138010 and 30370382). The costs of publication of this article were defrayed in part by the payment of page charges. This article must therefore be hereby marked "*advertisement*" in accordance with 18 U.S.C. Section 1734 solely to indicate this fact.

[1] To whom correspondence should be addressed. Tel.: 86-10-6488-8574; Fax: 86-10-6487-1293; E-mail: shenxun@sun5.ibp.ac.cn.

[2] The abbreviations used are: MAPK, mitogen-activated protein kinase; MKK, MAPK kinase; FRET, fluorescence resonance energy transfer; FLIM, fluorescence lifetime imaging microscopy; CFP, cyan fluorescent protein; YFP, yellow fluorescent protein; GFP, green fluorescent protein; PI3K, phosphatidylinositol 3-kinase; MK2, MAPK-activated protein kinase-2; Akt, serine/threonine kinase; Hsp27, heat shock protein 27; AA, arachidonic acid; LMB, lemptomycin B; MEF, mouse embryonic fibroblast; ATF-2, activating transcription factor-2; siRNA, small interference RNA; JNK, c-Jun N-terminal kinase; MAPKAPK, MAPK-activated protein kinase.

from the complex depends on the p38 kinase, because p38 is also activated by *N*-formyl-methionyl-leucyl-phenylalanine (25, 26). In other words, it has not been fully understood how the complex dissociates in the cells under different stimulation.

In this report, as a simplified model system, we studied the complex by directly observing the interaction between p38 kinase and hsp27 in intact live cells under a confocal laser-scanning microscope. Both FRET approach and immunoprecipitation analysis were used to investigate how the interaction was regulated. FRET represents direct radiation-less energy transfer from an excited donor fluorophore to an acceptor fluorophore and occurs when the two fluorophores are very close, usually in 6 nm. Owing to its extreme sensitivity to distances, it has become a powerful method in measuring protein-protein interactions in living cell (27–29). In this study, the cyan fluorescent protein (CFP)-fused hsp27 and the yellow fluorescent protein (YFP)-fused p38 MAPK were co-transfected transiently in mouse fibroblast cells, the interaction between these two chimeras was mainly observed by lifetime-based FRET. Together with immunoprecipitation studies, our results demonstrated that the interaction of hsp27 with p38 is mediated by MK2 and negatively regulated by phosphorylation of hsp27 that is induced by activation of either p38 or Akt.

EXPERIMENTAL PROCEDURES

Materials

The pECFP-C1 and pEYFP-C1 vectors were obtained from Clontech (Mountain View, CA). pKS2711 and pKS2711-3A vectors expressing wild-type human hsp27 and mutated hsp27 (serines 15, 78, and 82 substituted with alanine) were kindly provided by Prof. L. A. Weber (Dept. of Biology, University of Nevada, Reno, VA). Protein A was purchased from Pierce. The p38 MAPK Assay kit and mouse monoclonal anti-p38, rabbit anti-MAPKAPK-2, anti-phospho-p38(Thr-180/Tyr-182), anti-phospho-Akt(Ser-473), and anti-human phospho-hsp27 (Ser-82) antibodies were obtained from Cellular Signaling Technology (Beverly, MA). Rabbit polyclonal anti-human/mouse Hsp27, mouse anti-GFP, goat polyclonal anti-Akt1/2 antibodies, normal goat, and mouse IgG were obtained from Santa Cruz Biotechnology (Santa Cruz, CA). SB203580, wortmannin, arachidonic acid (AA), and lemptomycin B (LMB) were purchased from Sigma.

Construction of Fluorescent Chimeras

cDNAs of hsp27 and p38 were obtained by PCR amplification from pKS2711 and pcDNA3-FLAG-p38 constructs respectively. Subcloning hsp27 cDNA into CFP-expressing vector, pECFP-C1, in EcoRI-BamHI sites, made the CFP-hsp27 fusion construct. The p38 cDNA was subcloned into YFP-expressing vector, pEYFP-C1, in Hind-XhoI sites to construct the YFP-p38 fusion protein expression vector. A glycine was inserted between YFP and p38 as linker in the chimera. pECFP-hsp27-3A and pEYFP-p38AGF mutant constructs were made using the QuikChange site-directed mutagenesis kit from Stratagene (La Jolla, CA). The entire cDNA inserts were confirmed by DNA sequencing. The mutation points are Ser-15 → Ala, Ser-78 → Ala, and Ser-82 → Ala for Hsp27 and Thr-180 → Ala and Tyr182 → Phe for p38. The vectors pcDNA3.0-hsp27 and pcDNA3.0-hsp27-3A were constructed by subcloning hsp27 cDNA and hsp27-3A cDNA, respectively, from pKS2711 and pKS2711–3A into pcDNA3.0 in EcoRI-BamHI sites.

Cell Culture and Transfection

The mouse embryonic fibroblast (MEF) $MK2^{-/-}$ cells from MK2 knock-out mice and its wild-type control cells (MEF $MK2^{+/+}$) were kindly provided by Prof. M. Gaestel (Medical School Hanover, Germany) (30). These cells and mouse fibroblast L929 cells were maintained in Dulbecco's modified Eagle's medium containing 10% fetal calf serum at 37 °C in a CO_2 incubator. For FRET experiments L929 or MEF cells were co-transfected with a total of 1 μg of DNA plasmids (CFP to YFP constructs ratio was 1:2) using Lipofectamine 2000 (Invitrogen). Cells were grown in CO_2 incubators at 37°C for 20 h before FRET observation. To analyze the kinase activity of YFP-p38 and YFP-p38AGF, cells were transfected using the GenePulser II electroporation system (Bio-Rad) under the conditions of 500 V and 14-ms single pulse duration. The transfection efficiency was ~30%. For analysis of hsp27 phosphorylation in the cells expressing hsp27 or hsp27-3A, the cells were stably transfected with pcDNA3.0-hsp27 and pcDNA3.0-hsp27-3A using Lipofectamine 2000 and selected with 400 μg/ml G418.

Conventional Fluorescence Microscopy

An Olympus IX71 invert microscope equipped with the AquaCosmos Microscopic Image Acquisition and Analysis system (Hamamatsu Photonics K.K.) was used to observe the heat shock resistance of cells.

Fluorescence Resonance Energy Transfer Microscopy

Both intensity-based and lifetime-based FRET microscopy were used. The former was used as a more straightforward approach to demonstrate existence of the energy transfer between CFP-hsp27 and YFP-p38. However, most of FRET data were obtained using fluorescence lifetime imaging microscopy.

Intensity-based FRET Microscopy—All FRET observations were performed on a Leica DM IRE2 confocal laser scanning microscope system at 37 °C 20 h after cells were transfected. Excitation was provided by multimode argon ion laser beam using a double 458/514 nm diachronic splitter. Donor (CFP) was excited at 458 nm, and its fluorescence was detected in a bandwidth of 478–498 nm (CFP channel), whereas the excitation at 514 nm and emission at 545 ± 15 nm were used for detecting acceptor (YFP) (YFP channel). FRET was detected at the excitation of 458 nm and the emission of 545 ± 15 nm (FRET channel). Fluorescence images of the transfected cells were taken up at CFP-, YFP- and FRET channel sequentially. The net FRET signal was corrected against bleed-through of the non-FRET CFP and YFP fluorescence excited directly by 458 nm according to Equation 1 (31),

$$\text{Net FRET signal} = \text{FRET signal} - A \times \text{YFP signal} - B \times \text{CFP signal} \quad \text{(Eq. 1)}$$

where coefficients *A* and *B* represent the ratios of FRET signal to YFP signal in the absence of CFP-hsp27 and FRET signal to the CFP signal in the absence of the YFP-p38, respectively.

Dequenching of donor fluorescence by photobleaching of acceptor YFP was performed by illuminating the transfected cells at the YFP excitation wavelength (514 nm) for 2 min with full laser power, then CFP-hsp27 images were taken up at the same focal plane. FRET efficiency was calculated by using Equation 2,

$$E = 1 - (F_{DA}/F_D) \quad \text{(Eq. 2)}$$

where F_{DA} and F_D are the fluorescence intensity of CFP in the cells expressing both donor and acceptor, and donor alone, respectively. Application of photobleaching to the cell expressing CFP alone showed an apparent 9.8 ± 1.9% ($n = 6$) increase in CFP signal. This non-FRET increase may be attributed to a possible photoactivation of CFP by the 514 nm bleaching light and should be subtracted from the FRET efficiency values reported. Therefore, the FRET value reported by acceptor photobleach is a relative estimation that serves to confirm FRET data from the lifetime-based approach.

Fluorescence Lifetime Imaging Microscopy

Time-correlated single-photon counting fluorescence lifetime imaging was performed to obtain CFP fluorescence lifetime images in the cells transfected with CFP-hsp27 chimera alone or co-transfected with both CFP-hsp27 and YFP-p38 chimeras. This was carried out with a multiphoton confocal laser scanning microscope system (Leica DM IRE2 and Becker & Hickl SPC730). The femtoseconds pulsed laser (Coherent Mire 900) beam at 820 nm was used to excite donor CFP in the transfected cells. The two-photon excited fluorescence was detected with a 480 ± 30 nm band-pass filter (Chroma, Rockingham, VT). The laser power was adjusted to give an average photon-counting rate of 10^4–10^5 photons s^{-1} without detectable photobleaching of the samples. The cells with moderate fluorescence intensity were picked for observation to avoid any possible artifact caused by too much overexpression. Each fluorescence lifetime imaging microscopy (FLIM) image of the cells was taken for 50 s and continued for 30 min at 5-min intervals. Data were collected and analyzed by software provided by the manufacturer. Two-exponential decay dynamics was applied to analyze fluorescence decay characteristics of CFP and to calculate its fluorescence lifetime at each pixel. The FRET efficiency was calculated by using Equation 3,

$$E = 1 - (T_{DA}/T_D) \quad \text{(Eq. 3)}$$

where T_{DA} and T_D are the mean fluorescence lifetimes of CFP in the cells expressing donor plus acceptor and donor alone, respectively.

Immunoprecipitation Analysis

Non-transfected or transfected cells were lysed for 10 min on ice in the lysis buffer containing 20 mM Tris (pH 7.5), 150 mM NaCl, 1 mM EDTA, 1 mM EGTA, 1% Triton X-100, 2.5 mM sodium pyrophosphate, 1 mM β-glycerolphosphate, 1 mM Na_3VO_4, 1 μg/ml leupeptin, and 1 mM phenylmethylsulfonyl fluoride. Following centrifugation at 14,000 × *g* for 10 min at 4 °C, one aliquot of clear lysate was incubated with 5 μl of mouse monoclonal anti-p38 antibody or 5 μl of goat polyclonal anti-Akt1/2 antibody, while another aliquot of the clear lysate was incubated with 5 μl of normal mouse IgG or normal goat IgG overnight with continuous rotation at 4 °C. The latter was used for control experiments to examine nonspecific interaction. Protein A-Sepharose beads (30 μl) were then added, and the samples were gently rocked for an additional 3 h at 4 °C. After five washes by centrifugation in lysis buffer, the beads were resuspended in 30 μl of 2× SDS sample buffer (4% SDS, 0.25 M Tris-HCl, 10% glycerol, and 0.02% bromophenyl blue, pH 6.8), and then boiled for 5 min. The proteins dissociated from the beads were separated by 10% SDS-PAGE, transferred onto nitrocellulose membrane, and blocked with 5% nonfat milk in TBS/T buffer (20 mM Tris base, 135 mM NaCl, 0.1% Tween 20, adjust to pH 7.6 with HCl) for 1 h. The blots were probed sequentially by anti-hsp27 and anti-p38 bodies in the precipitate with anti-p38 antibody, or probed sequentially by anti-GFP, rabbit anti-Akt, and anti-MK2 antibodies (1:1000) in the precipitate with goat anti-Akt1/2 antibodies and finally with peroxidase-conjugated secondary antibody in 5% nonfat milk in TBS/T buffer after removal of the free primary antibodies. Specific protein bands were visualized by chemiluminescence.

Assay of p38 Kinase Activity

p38 activity was assayed by measuring the ability of immunoprecipitated phospho-p38 to phosphorylate activating transcription factor-2 (ATF-2) using the p38 MAPK assay kit. Briefly, untreated and H_2O_2-exposed cells were lysed with 500 μl of above-mentioned lysis buffer. Following centrifugation at 10,000 × *g* for 10 min at 4°C, cleared lysates were incubated with 30 μl of immobilized phospho-p38 monoclonal antibody bead with gentle rocking overnight at 4°C. The beads were washed twice with lysis buffer and twice with 1× kinase buffer containing 25 mM Tris (pH 7.5), 5 mM β-glycerolphosphate, 2 mM dithiothreitol, 0.1 mM Na_3VO_4, 10 mM $MgCl_2$, and then incubated with 50 μl 1 × kinase buffer supplemented with 200 μM ATP and 1 μl of ATF-2 at 30 °C for 30 min. The reaction was terminated by addition of 25 μl of 3× SDS sample buffer (containing 187.5 mM Tris-HCl (pH 6.8), 6% w/v SDS, 30% glycerol, 150 mM dithiothreitol, 0.03% w/v bromphenol blue). 30 μl of each sample was separated by SDS-PAGE, and the phosphorylated ATF-2 was detected by immunoblotting using anti-phospho-ATF-2 antibody supplied with the kit.

Knockdown of Akt and p38 by siRNA

The validated target sequences were: 5′-UGCCCUUCUACAACCAGGA-3′, 5′-UACCGAGAGUUGCGUCUGC-3′, 5′-UACCGUGAGCUGCGCCUAC-3′, and 5′-UUCUCCGAACGUGUCACGU-3′ for mouse Akt1 siRNA (32), mouse p38α siRNA (33), mouse p38β siRNA (33), and mock siRNA, respectively. They were chemically synthesized by GenePharma Co. (Shanghai, China). Cells were seeded in 6-well plates and incubated overnight, then transfected with 100 nM siRNA for 12 h using 2 μl of VigoFect (Vigorous Biotechnology, Beijing) per well. The expression of Akt and p38 in the transfected cells was assayed by Western blotting using goat anti-Akt1/2 and rabbit anti-p38 polyclonal antibody, respectively, 36 h after transfection.

Determination of Phosphorylated p38 MAPK, hsp27, and Akt

Phosphorylation of p38, hsp27, and Akt was determined using corresponding phospho-specific antibodies. Cells exposed to H_2O_2 or AA were lysed with 1× SDS sample buffer on ice. Then, the lysate was sonicated for 20 s on ice to shear DNA and reduce viscosity. The samples were boiled for 5 min and electrophoresed in 10% SDS-PAGE gel. Immunoblotting was performed with anti-phospho-p38, anti-phospho-hsp27, and anti-phospho-Akt antibodies, respectively.

Statistics

The fluorescence lifetime of CFP-hsp27 shown on each image is the average for whole cells. The FRET efficiency was calculated based on the fluorescence lifetimes obtained from three independent imaging of different single cells. In statistical analysis of the phosphorylation level of p38 and Akt obtained from Western blotting measurement, the average value and standard deviation was calculated based on three independent measurements.

RESULTS

CFP-tagged Hsp27 Still Protects the Transfected L929 Cells from Heat Shock-induced Death—To examine if the CFP-tagged hsp27 still functions as a stress-response protein, the cells transiently transfected with either pECFP-hsp27 or pECFP-hsp27-3A and the non-transfected wild-type cells were subjected to heat shock at 44 °C for 30 min and imaged 30 h later. As Fig. 1*A* shows, only those fluorescent CFP-hsp27-expressing cells survived from the heat shock, whereas almost all non-fluorescent wild-type cells died. The result indicates that CFP-tagged hsp27 still protects the cells from heat shock-induced death (see *upper panel*). In contrast, expression of CFP-fused dominant negative mutant of hsp27 (CFP-hsp27-3A) failed to prevent cell death (see *lower panel*), indicating that hsp27-3A, in which the residues Ser-15, Ser-78, and Ser-82 are mutated to alanines, is a functionally dead mutant.

YFP-tagged p38 Has Normal Function of p38 MAPK—To examine if the YFP-tagged p38 is still a functional kinase, its ability to phosphorylate ATF-2, the substrate of p38 kinase, was checked. The cells were transiently transfected with pEYFP-p38 or pEYFP-p38AGF by electroporation. Immunoprecipitation analysis was performed with anti-p38 antibody in wild-type and transfected cells either unexposed or exposed to 1 mM H_2O_2 for 30 min, and the immunoprecipitate was then used to phosphorylate ATF-2. As Fig. 1*B* shows, H_2O_2 activated p38 in all three types of cell, but the highest activation was detected in the pEYFP-p38-transfected cells. It was also noticed that the H_2O_2-induced p38 activation in the cells transfected with YFP-p38AGF, the mutant that is unable to be phosphorylated, was much weak than that in wild-type cells. The results indicate that YFP-tagged p38 still functions as MAPK, whereas the YFP-p38AGF acts as a competitor to suppress activation of the endogenous p38 kinase in the cells.

The CFP-hsp27 and YFP-p38 Still Form a Complex with MK2 and Akt in the Transfected Cells—To justify the FRET study on the interaction of YFP-p38 with CFP-hsp27 as a suitable approach to study the signaling complex consisting of p38 kinase, Akt, MK2, and hsp27, it should be checked if the fusion

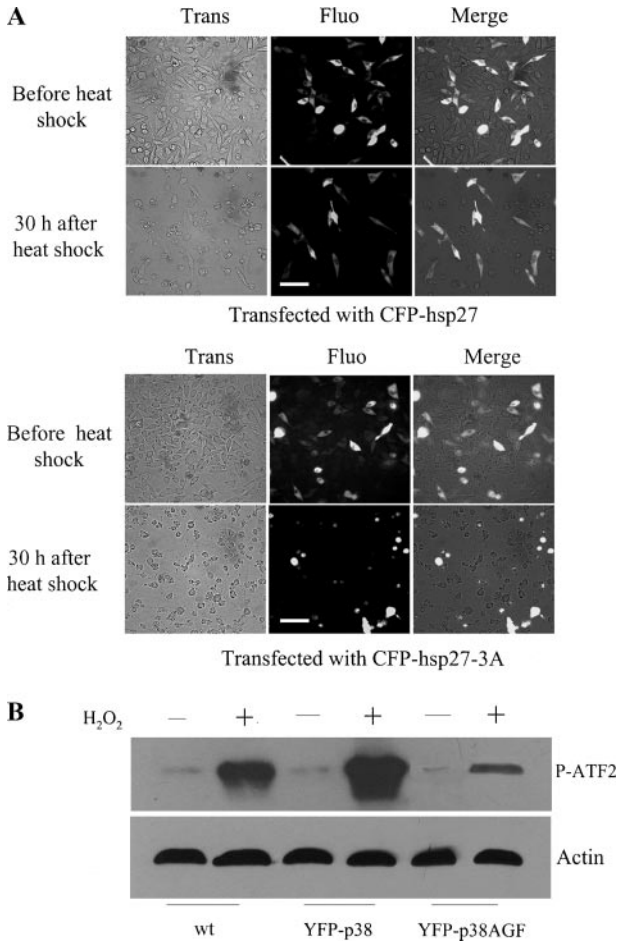

FIGURE 1. **Heat shock-induced death of L929 cells transfected with CFP-hsp27 or CFP-hsp27-3A and H_2O_2-induced activation of p38 kinase in wild-type and YFP-p38- or YFP-p38AGF-transfected L929 cells.** *A*, cells were transiently transfected with pECFP-hsp27 (*upper panel*) or pECFP-hsp27-3A (*lower panel*) for 20 h and then subject to heat shock for 30 min at 44 °C. Phase contrast and fluorescence images of the cells were taken before the heat shock and 30 h after. The fluorescent cells represent the cells expressing CFP-hsp27 or CFP-hsp27-3A. *B*, cells were transiently transfected with pEYFP-p38 and pEYFP-p38AGF and cultured for 24 h before exposure to 1 mM H_2O_2 for 30 min. Then, p38 activity was measured as phosphorylation of its substrate ATF-2. The wild-type cells with or without exposure to H_2O_2 were used as controls. The *scale bars* on micrograms are 32 μm.

proteins, CFP-hsp27 and YFP-p38, are part of the complex. Therefore, to see if the fusion proteins are associated with Akt and MK2, immunoprecipitation analysis was performed with either anti-Akt1/2 antibody or the normal IgG in lysate of the cells transiently co-transfected with pEYFP-p38 and pECFP-hsp27. The results are shown in Fig. 2*A*. The immunoblot probed by anti-GFP antibody in lysate of the cells transfected with CFP-hsp27 or YFP-p38 showed clear existence of CFP or YFP at the position corresponding to CFP-hsp27 or YFP-p38 (see *lanes 2* and *3*). Analysis of the immunoprecipitate with anti-Akt1/2 antibody from lysate of the CFP-hsp27/YFP-p38-co-transfected cells clearly showed that CFP-hsp27, YFP-p38, and MK2 were complexed with Akt (see *lane 5*). Immunoprecipitation of the cell lysate with normal IgG followed by Western blot analysis with anti-GFP and anti-MK2 antibodies revealed no detectable association of these proteins, indicating the specificity of Akt interactions with p38, hsp27, and MK2 (see *lanes 4*, *6*, and *8*). It was found that even YFP-fused p38

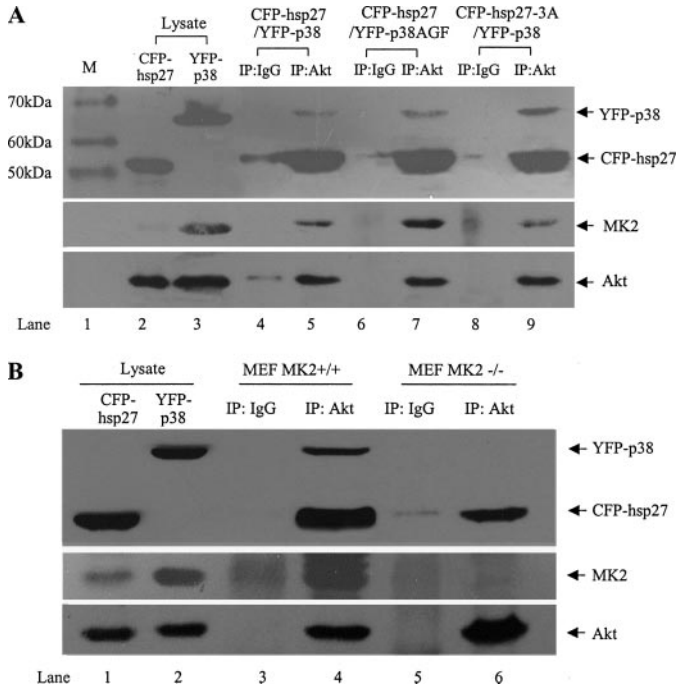

FIGURE 2. **Analysis of the CFP- and YFP-fused proteins in the immunoprecipitate with either goat anti-Akt1/2 antibody or normal goat IgG in the lysates from the transfected L929, MEF MK$^{+/+}$ and MEF MK2$^{-/-}$ cells.** *A*, immunoblot of CFP-fused proteins, YFP-fused proteins, MK2, and Akt probed sequentially by anti-GFP, anti-MK2, and rabbit anti-Akt antibodies in the immunoprecipitates from the lysates of the L929 cells co-transfected either with CFP-hsp27/YFP-p38, or CFP-hsp27/YFP-p38AGF, or CFP-hsp27-3A/YFP-p38 for 40 h. Either CFP-fused hsp27 and its mutant (hsp27-3A) or YFP-fused p38 and its mutant (p38AGF), as well as MK2 were all associated with Akt (*lanes 5*, *7*, and *9*). The immunoblots of CFP-hsp27 and YFP-p38, probed by anti-GFP antibody in the lysate of the cells transfected with either CFP-hsp27 or YFP-p38, were used as control (*lanes 2* and *3*). *Lane 1* shows various protein markers. *B*, immunoblot for CFP-hsp27, YFP-p38, MK2, and Akt probed sequentially by anti-GFP, anti-MK2, and rabbit anti-Akt antibodies in the immunoprecipitates from the lysate of the MEF MK2$^{+/+}$ cells and MEF MK2$^{-/-}$ cells. CFP-fused hsp27 is complexed with Akt in both cell types (*lanes 4* and *6*). YFP-p38 and MK2 were complexed with Akt only in MEF MK$^{+/+}$ cells (*lane 4*) but not in MEF MK$^{-/-}$ cells (*lane 6*). The immunoblot of CFP-hsp27 and YFP-p38, probed by anti-GFP antibody in lysate of the MEF MK$^{+/+}$ cells transfected with either CFP-hsp27 or YFP-p38, was used as control (*lanes 1* and *2*).

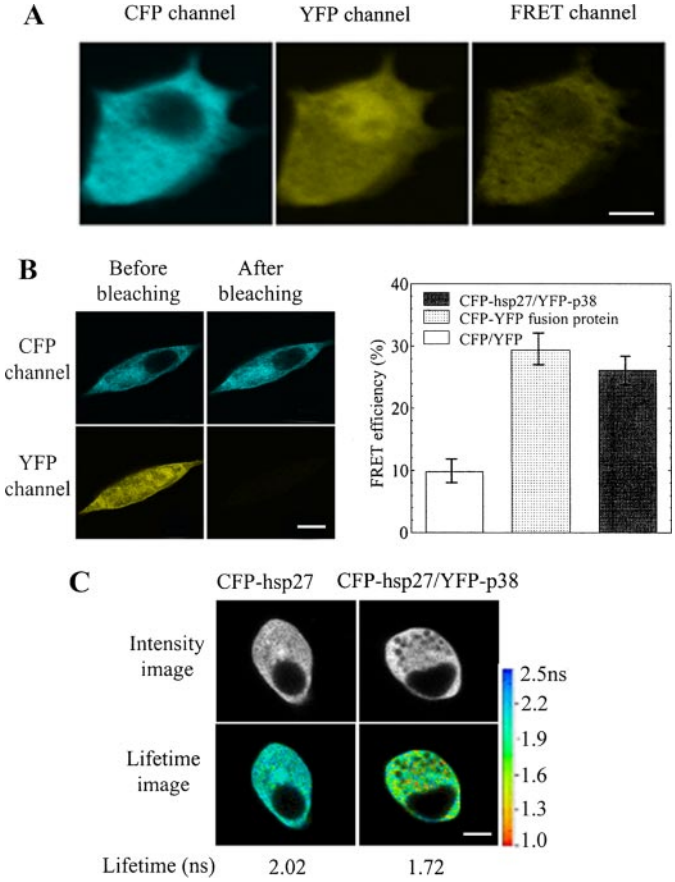

FIGURE 3. **Fluorescence intensity and lifetime images of L929 cells transfected with CFP-hsp27 and YFP-p38, separately or in combination for 20 h.** *A*, fluorescence intensity image of the cells co-transfected with CFP-hsp27 and YFP-p38 taken in CFP, YFP, and FRET channels, respectively. The fluorescence in FRET channel was corrected against bleed-through of the non-FRET CFP and YFP fluorescence excited at 458 nm. *B*, fluorescence intensity images of the cells co-transfected with CFP-hsp27 and YFP-p38 in CFP and YFP channels before and after photobleaching of YFP. An increase of the CFP fluorescence and dramatic decrease of the YFP fluorescence were observed after the photobleaching. The attached histogram shows the FRET efficiency from CFP to YFP in the cells transfected with both CFP-hsp27 and YFP-p38, CFP-YFP fusion protein and both of CFP and YFP, respectively. *C*, the intensity (*upper panel*) and lifetime images (*lower panel*) of the cells transfected with CFP-hsp27 alone and the cells co-transfected with both CFP-hsp27 and YFP-p38 at two-photon excitation of 820 nm laser beam. The *scale bars* on the micrograms are 8 μm.

mutant (YFP-p38AGF) and CFP-fused hsp27-3A were also in the complex (see *lanes 7* and *9*). The immunoprecipitation analysis demonstrates that fusion with fluorescent protein does not prevent hsp27 and p38 from forming a complex with Akt and MK2.

Same as in L929 cells, analysis of the immunoprecipitate with anti-Akt1/2 antibody in the lysate of the MEF MK2$^{+/+}$ cells co-transfected with both CFP-hsp27 and YFP-p38 clearly showed that CFP-hsp27, YFP-p38, and MK2 were complexed with Akt (see *lane 4* in Fig. 2*B*). However, YFP-p38 could not be detected in the precipitate with anti-Akt1/2 antibody in the MEF MK2$^{-/-}$ cells co-transfected with both CFP-hsp27 and YFP-p38 (*lane 6* in Fig. 2*B*). The nonspecific binding of the probed proteins was also checked by the immunoprecipitation with IgG (*lanes 3* and *5* in Fig. 2*B*).

Interaction of p38 and hsp27 in Quiescent L929 Cells—Although association of hsp27 with p38 has been demonstrated by immunoprecipitation studies, direct observation of the interaction between these two proteins in intact living cell has not been reported. To conduct such an observation, cells were co-transfected with pECFP-hsp27 and pEYFP-p38. After incubation for 20 h in a CO_2 incubator, the cells were imaged on a Leica DM IRE2 confocal laser-scanning microscope thermostatted at 37 °C. The cells co-expressing CFP-hsp27 and YFP-p38 were selected based on double-colored fluorescence. Fig. 3*A* shows the fluorescence image of cells in CFP, YFP, and FRET channels, respectively. CFP-hsp27 was localized in cytoplasm, whereas YFP-p38 was localized in whole cell but preferably in nucleus. The fluorescence from cytoplasm was clearly detected in the FRET channel after correction for bleed-through of CFP and YFP, indicating a direct interaction between p38 and hsp27 in living cells.

To verify energy transfer from the excited hsp27-fused CFP to the p38-fused YFP, the acceptor YFP was photobleached, and the fluorescence intensity of the donor CFP was measured before and after the photobleaching. As Fig. 3*B* shows, no fluorescence could be detected in the YFP channel, and the fluores-

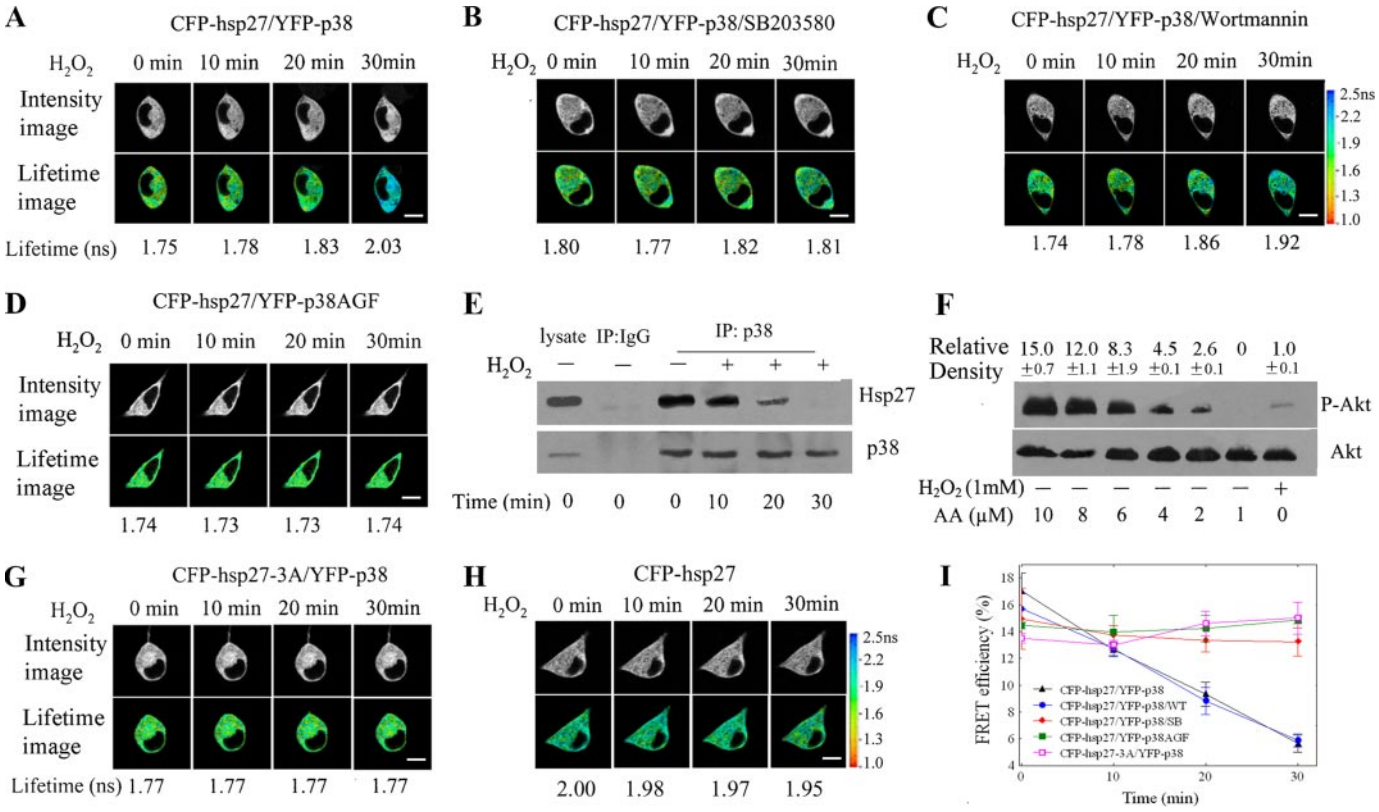

FIGURE 4. **H_2O_2-induced activation of p38 kinase dismisses the interaction of p38 with hsp27.** The fluorescence lifetime of L929 cells co-transfected with various combinations of CFP- and YFP-based chimeras were imaged after exposure to H_2O_2 (1 mM). *A*, co-transfection with CFP-hsp27 and YFP-p38 in cells. *B*, cell co-transfected with CFP-hsp27 and YFP-p38 in the presence of 2 μM SB203580. *C*, co-transfection with CFP-hsp27 and YFP-p38 in the presence of 100 nM wortmannin. *D*, co-transfection with CFP-hsp27 and YFP-p38AGF. *E*, the precipitated hsp27 with anti-p38 antibody or normal mouse IgG in wild-type L929 cells at various times after exposure to 1 mM H_2O_2. The p38 contents in the precipitates were used as control. *F*, immunoblot of the phosphorylated Akt (at Ser-473) in the wild-type L929 cells either stimulated by AA at various concentrations or exposed to 1 mM H_2O_2 for 30 min. The activities of Akt calculated based on three independent assays are shown as relative densities of the blots (the values above the blots). *G*, the cell co-transfected with CFP-hsp27-3A and YFP-p38. All images were taken 20 h after transfection, and the lifetimes indicated are mean values over all pixels within cytosol. *H*, transfection with CFP-hsp27 alone in cell. *I*, the calculated FRET efficiencies from CFP donor to YFP acceptor in all above five cases at indicated times after the cells were exposed to H_2O_2. All data are the means of three independent measurements with ± S.D. indicated by *error bars*. The *scale bar* for each group of micrograms is 8 μm.

cence in the CFP channel increased after the p38-fused YFP was photobleached. The energy transfer efficiency from CFP to YFP was calculated based on the ratio of the cytoplasmic CFP fluorescence intensity of the cell before photobleaching of the YFP to that after photobleaching. The efficiency of 16% was obtained using Equation 2 and corrected for the increase in CFP signal caused possibly by the bleaching light-induced photoactivation, which was 9.8 ± 1.9% based on six measurements (see the *open column* on the histogram in Fig. 3*B*).

Furthermore, FLIM was also performed to see the fluorescence energy transfer from CFP-hsp27 to YFP-p38. Because fluorescence lifetime is independent of light path and chromophore concentration, it is thus well suited for studies in intact cells. FRET leads to a shortening of the fluorescence lifetime of donor. As shown in Fig. 3*C*, the fluorescence lifetime of CFP-hsp27 was measured as 2.02 in the absence of YFP-p38 acceptor, but shortened to 1.72 ns in the presence of YFP-p38, indicating occurrence of FRET between these two chimeras. The mean FRET efficiency was calculated as (15.7 ± 2.5)% (n = 6) using Equation 3. It was noticed that the efficiency obtained from the lifetime-based measurement was quite close to that obtained from the intensity-based measurement.

Activation of p38 MAPK Disrupts Its Interaction with hsp27—As described under "Experimental Procedures," shortening of the fluorescence lifetime of hsp27-fused CFP in the presence of p38-fused YFP is used as an indication of the interaction between these two chimeras. To check if dimerization of hsp27 could affect the fluorescence lifetime of CFP-hsp27, the fluorescence lifetime of CFP-hsp27 was monitored in the absence of the YFP-p38 acceptor in the cells exposed to H_2O_2. It turned out that almost no effect of the dimerization on the fluorescence lifetime could be detected (see Fig. 4*H*).

The lifetime of the hsp27-fused CFP in the presence of YFP-p38 is markedly shorter than that of the CFP-hsp27 in the cells without co-transfection of YFP-p38 when cell was not exposed to H_2O_2 (compare Fig. 4, *A* and *H*). This indicates that hsp27 directly interacts with p38 in normal growing cells under no stress. How would such an interaction be affected when cells are subjected to oxidative stress? We thus monitored kinetically the FRET between CFP-hsp27 and YFP-p38 in the cells during exposure to H_2O_2. As Fig. 4*A* shows, the fluorescence lifetime of hsp27-fused CFP gradually increased from 1.75 to 2.03 ns within 30 min in a single living cell. Meanwhile, the FRET efficiency between the two chimeras decreased from (17.0 ± 1.3)%

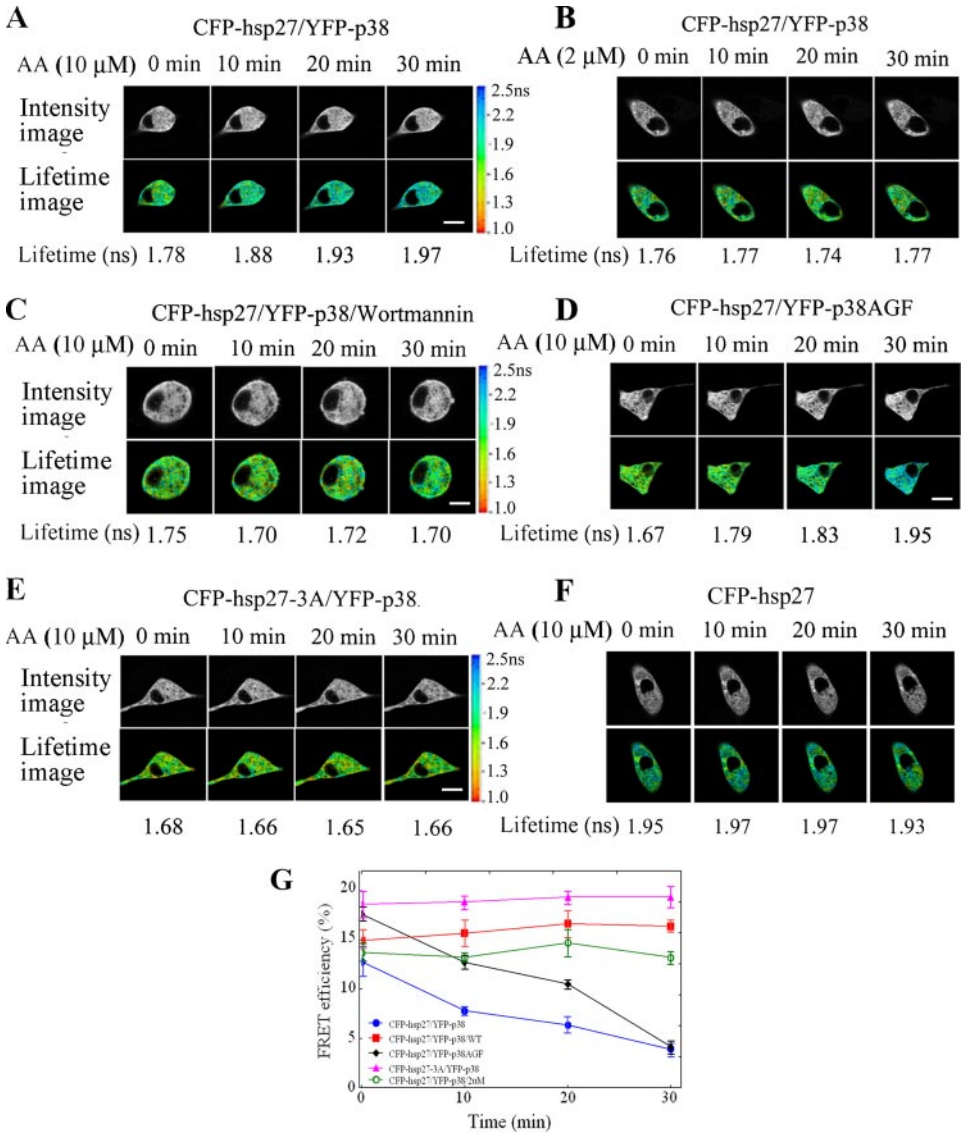

FIGURE 5. **Activation of Akt by AA dismisses the interaction of p38 with hsp27.** The fluorescence lifetime images of L929 cells co-transfected with various combinations of CFP- and YFP-based chimeras at indicated times after AA (*AA*) stimulation. *A* and *B*, co-transfection with CFP-hsp27 and YFP-p38 and stimulated with 10 and 2 μM AA, respectively. *C*, co-transfection with CFP-hsp27 and YFP-p38 and stimulated by 10 μM AA in the presence of 100 nM wortmannin. *D*, co-transfection with CFP-hsp27 and YFP-p38AGF. *E*, co-transfection with CFP-hsp27-3A and YFP-p38. In all cases, the images were taken 20 h after transfection, and the lifetimes indicated are mean values over all pixels in cytosol. *F*, transfection with CFP-hsp27 alone and stimulated by 10 μM AA. *G*, the calculated FRET efficiencies from CFP donor to YFP acceptor in all cases at indicated times after the stimulation. All data are the means of three independent measurements with ± S.D. indicated as *error bars*. The *scale bar* on the micrograms is 8 μm.

to (5.6 ± 0.6)% (see Fig. 4*I*). These data indicate that the interaction between CFP-hsp27 and YFP-p38 becomes weaker and weaker and finally disappears within 30 min after H_2O_2 exposure. As a parallel experiment, the p38 activity was found gradually increased in cells upon exposure to H_2O_2 (see Fig. 6*A*). Thus, disappearance of the interaction between hsp27 and p38 may be linked to p38 activation. Immunoprecipitation study showed that the p38-associated hsp27 also diminished within 30 min in wild-type L929 cells after H_2O_2 exposure, exhibiting the same tendency as observed in FRET measurements (Fig. 4*E*).

To further verify that the disappearance of the interaction between these two proteins is attributed to activation of p38, SB203580, the selective inhibitor of p38 (34, 35), was used to inhibit p38 activation in the H_2O_2-exposed cells and to see if the interaction could be maintained. As Fig. 4*B* shows, H_2O_2 could no longer dispel the interaction of CFP-hsp27 with YFP-p38 as indicated by unaffected fluorescence lifetime of the donor and FRET efficiency in the presence of 2 μM SB203580. Because SB203580 may also block the phosphorylation and activation of Akt, which is another member of the signaling complex and able to dispel hsp27 from the complex by phosphorylation of hsp27 (20, 21), we checked if activation of p38 kinase still dismissed its interaction with hsp27 when Akt activation was inhibited by wortmannin, a selective PI3K inhibitor. The cells co-expressing CFP-hsp27 and YFP-p38 were exposed to 1 mM H_2O_2 in the presence of 100 nM wortmannin. The presence of wortmannin did not prevent the lifetime of the fluorescent CFP donor from gradual increase after exposure to H_2O_2, indicating that activation of p38 is enough for dismissing the interaction of hsp27 with p38 kinase even without the activation of Akt. The reasons for a diminished role of Akt in the H_2O_2-induced dismissal of p38 with hsp27 may be twofold. One is because of much more exogenous p38 and less endogenous Akt in the cells co-transfected with CFP-hsp27 and YFP-p38. The other reason may be the less efficacy of H_2O_2 in activating Akt. As Fig. 4*F* shows, the Akt activity induced by 1 mM H_2O_2 was only 1/15th the activity induced by 10 μM AA in the wild-type cells. In the next section, we will show that even 2 μM AA, which can induce an Akt activation that is 2.6-fold higher than that induced by 1 mM H_2O_2 in the cells, could not dispel the interaction between CFP-hsp27 and YFP-p38 (see Fig. 5*B*). Taking all these observations together, we may conclude that activation of p38 kinase is responsible for the dissociation of hsp27 from the complex in the cell exposed to H_2O_2.

To avoid any nonspecific effect of the pharmacological inhibitor, the vector expressing YFP-fused kinase-dead p38 mutant (p38AGF), which can no longer be phosphorylated and activated because of mutation at its dual phosphorylation motif (Thr-Gly-Tyr), was constructed and co-transfected with CFP-hsp27 into cells. Consistent with inhibitor experiment, the

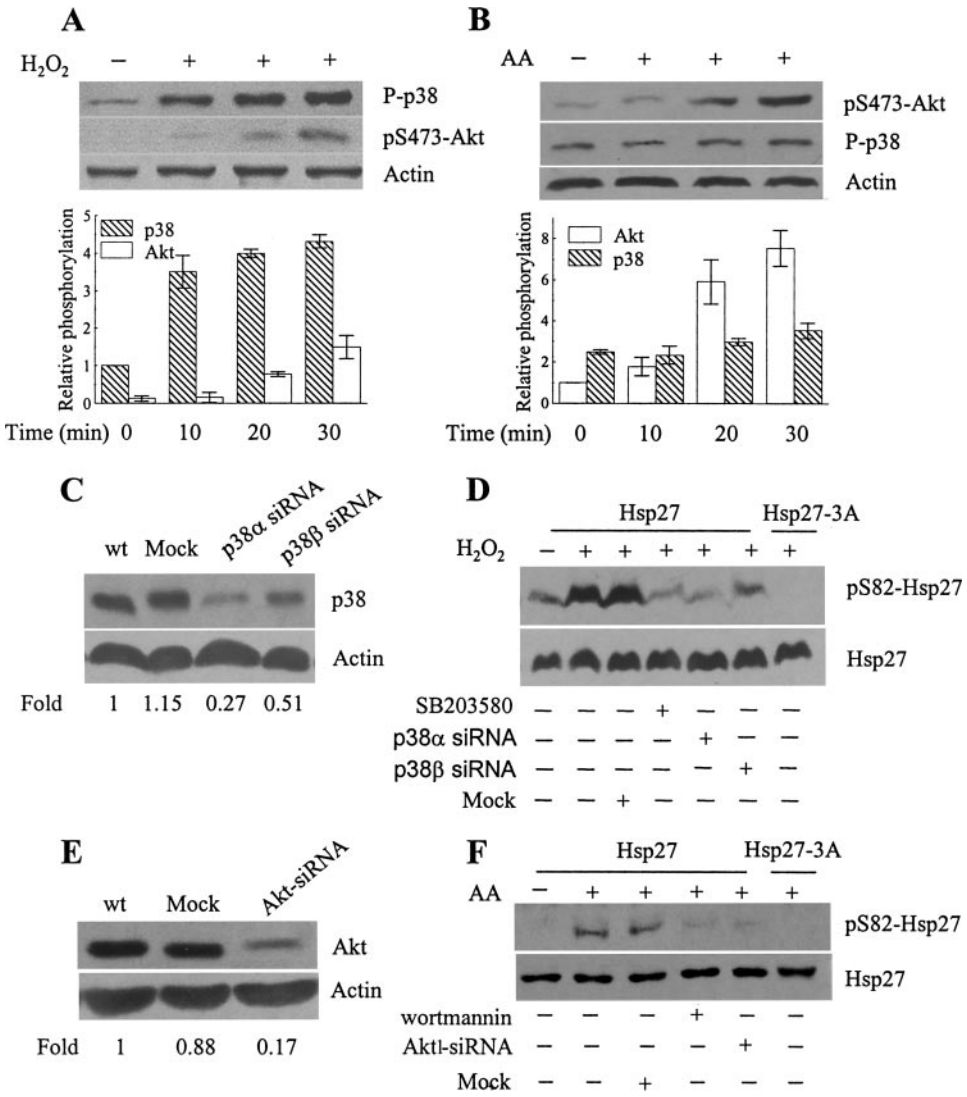

FIGURE 6. **Phosphorylation of p38, Akt, and Hsp27 in L929 cells exposed to H_2O_2 (1 mM) or stimulated by AA (10 μM).** *A*, immunoblot of the phosphorylated p38 and Akt (Ser-473) assayed at various indicated times in the cells after exposure to H_2O_2 for 30 min. The *histogram* shows the statistical analysis of three independent assays. *B*, immunoblot of the phosphorylated p38 and Akt (Ser-473) at various indicated times in the cells stimulated by AA for 30 min. The *histogram* shows the statistical analysis of three independent assays. *C*, expression level of p38 kinase in the wild-type cells, the cells transfected with 100 nM siRNA for p38α, siRNA for p38β, and scrambled oligonucleotide (*Mock RNA*), respectively, for 12 h. Western blotting was performed 36 h after transfection. *D*, immunoblot of the phosphorylated hsp27 (at Ser-82) in the cells stably transfected with hsp27 and its mutant hsp27-3A, respectively, and exposed to H_2O_2 for 30 min under various conditions: in the presence or absence of 2 μM SB203580 and transiently transfected, respectively, with 100 nM p38α siRNA, p38β siRNA, or the mock RNA for 12 h followed by 36 incubation. *E*, expression level of Akt in the wild-type cells, the cells transfected with 100 nM siRNA for Akt1, and scrambled oligonucleotide (*Mock RNA*), respectively, for 12 h. Western blotting was performed 36 h after transfection. *F*, immunoblot of the phosphorylated hsp27 (at Ser-82) in the cells stably transfected with hsp27 and its mutant hsp27-3A, respectively, and stimulated by AA for 30 min under various conditions: in the presence or absence of 100 nM wortmannin, and transiently transfected, respectively, with 100 nM Akt1 siRNA or the mock RNA for 12 h followed by 36-h incubation.

FLIM observation showed no change in the fluorescence lifetime of the hsp27-fused CFP when cells were co-transfected with YFP-tagged p38AGF and exposed to H_2O_2 (Fig. 4*D*). These results further demonstrate that activation of p38 is enough for disrupting the hsp27/p38 interaction in H_2O_2-exposed cells.

A remaining question is why activation of p38 leads to disruption of the interaction. Activation of p38 leading to phosphorylation of hsp27 may be a reasonable explanation. To verify this, CFP-fused dominant-negative mutant of hsp27 (pECFP-hsp27-3A) and YFP-tagged p38 were co-transfected into cells to see whether their interaction was affected by activation of p38. It was found that activation of p38 could no longer dispel the interaction of p38 with hsp27-3A (Fig. 4*G*). This observation suggests that the activated p38 can no longer affect the interaction of hsp27 with p38 when hsp27 is unable to be phosphorylated (see the *far-right lane* in Fig. 6*F*). The H_2O_2-induced kinetic changes of the FRET efficiency between CFP-hsp27 (or hsp27-3A) and YFP-p38 (or p38AGF) in single living cell under various conditions are calculated by Formula 2 and shown in Fig. 4*I*.

Activation of Akt Disrupts the Interaction of p38 and hsp27—To find out the possible role of Akt in regulating the interaction of p38 with hsp27, AA, an activator of PI3K-Akt signaling (36), was used to activate Akt, whereas wortmannin, a selective inhibitor of PI3K (37, 38), was used to inhibit AA-induced Akt activation. Immunoblotting analysis showed a significant activation of Akt in L929 cells stimulated by AA (see Fig. 6*B*). FLIM was performed to detect the interaction of hsp27 with p38 in the cell transfected with CFP-hsp27 and YFP-p38 after AA stimulation either in the absence or in the presence of wortmannin. As Fig. 5*A* shows, activation of Akt (phosphorylation at Ser-473) by 10 μM AA resulted in a gradual increase in the fluorescence lifetime of the donor CFP (from 1.78 to 1.97 ns) within 30 min, indicating a dissociation of CFP-hsp27 from YFP-p38. However, it seems that there is a threshold of AA concentration for Akt-regulated disruption of the interaction. As Fig. 5*B* shows, 2 μM AA stimulation was unable to dispel CFP-hsp27 from YFP-p38 in living cells. The CFP-hsp27 retained its association with p38 when wortmannin was present (Fig. 5*C*). The results well demonstrate that activation of Akt also leads to dissociation of hsp27 from p38. To exclude any possible role of p38 kinase in AA-stimulated cells, the interaction of CFP-tagged hsp27 with YFP-tagged kinase-dead p38 mutant (YFP-p38AGF) was detected by FLIM in the AA-stimulated cells. It turned out that the activation of Akt by AA also led to dissociation of hsp27 from p38 even under the condition that p38 is no longer acti-

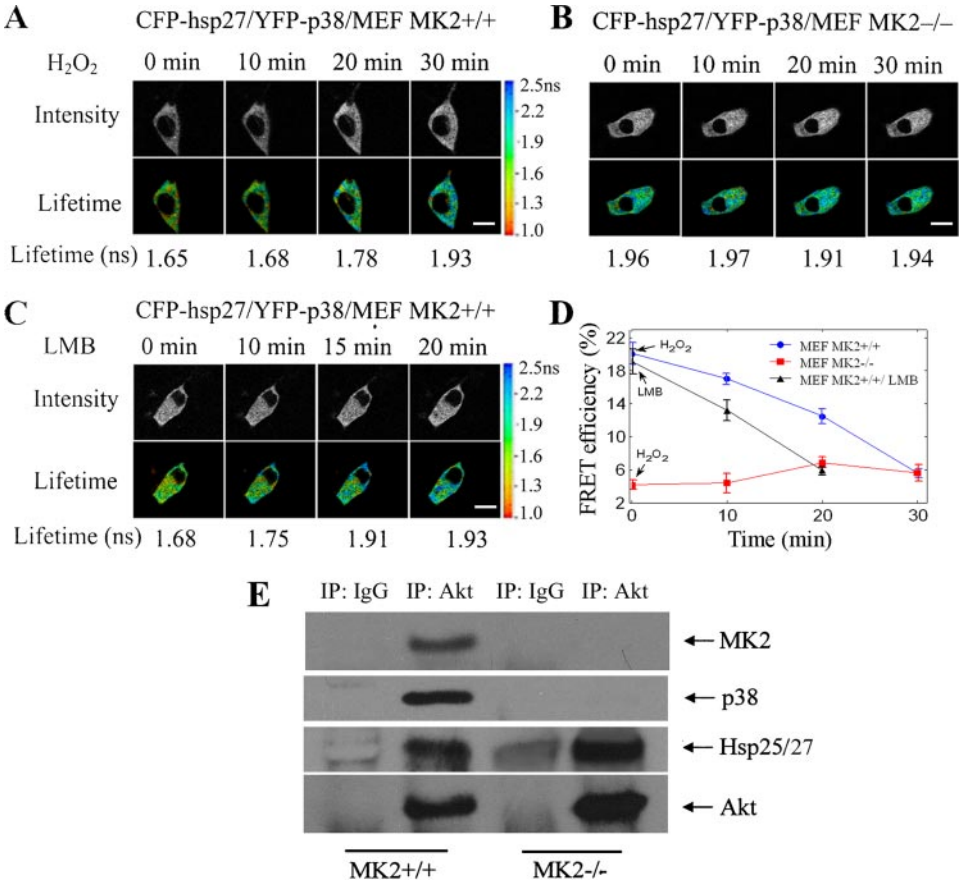

FIGURE 7. **MK2 regulation of the interaction between p38 and hsp27 in MEF cells.** *A* and *B*, fluorescence lifetime images of the MEF MK2$^{+/+}$ and MEF MK2$^{-/-}$ cells co-transfected with pEYFP-p38 and pECFP-hsp27 taken at indicated times after exposure to 1 mM H_2O_2 20 h after transfection. *C*, the fluorescence lifetime images of the MEF MK2$^{+/+}$ cell co-transfected with pEYFP-p38 and pECFP-hsp27 taken at various times after addition of 5 ng/ml LMB. *D*, the calculated time-dependent FRET efficiencies from the CFP donor to YFP acceptor in all above three cases. All data are the means of three independent measurements with ± S.D. indicated as *error bars*. The *scale bar* on each group of micrograms is 8 μm. *E*, immunoblot of p38, hsp27, MK2, and Akt probed sequentially by anti-p38, anti-hsp27, anti-MK2, and rabbit anti-Akt antibodies in the immunoprecipitate with goat anti-Akt1/2 antibody or normal goat IgG from lysate of MEF MK2$^{+/+}$ and MEF MK2$^{-/-}$ cells, respectively. p38, hsp27, and MK2 were found in the precipitate from MK2$^{+/+}$ cells, whereas only hsp27 was found in the precipitate from MK2$^{-/-}$ cells.

vated (Fig. 5*D*). This indicates that activation of Akt but not p38 is also responsible for the release of hsp27 from p38 in AA-stimulated cells. As a control, the fluorescence lifetime of hsp27-fused CFP in the cells transfected only with CFP-hsp27 was monitored under AA stimulation. No detectable change was observed during the stimulation (see Fig. 5*F*).

The same question as to why activation of Akt leads to disruption of the interaction between hsp27 and p38 may be asked. As Fig. 5*E* shows, replacement of hsp27 with its dominant-negative mutant in CFP-hsp27 chimera led to a sustaining interaction of the fusion protein, CFP-hsp27-3A, with YFP-p38, and even Akt was activated by 10 μM AA. Phosphorylation of hsp27 by activated Akt is a reasonable explanation for the dissociation of hsp27 from the complex in the living cell stimulated by AA. The AA-induced kinetic changes of the FRET efficiency between CFP-hsp27 (or hsp27-3A) and YFP-p38 (or p38AGF) in living cells under various conditions are calculated and shown in Fig. 5*G*.

Causal Relation between p38 or Akt Activation and hsp27 Phosphorylation—We have shown that mutation of the phosphorylation sites in hsp27 prevents dissociation of hsp27 from p38 whether p38 or Akt is activated or not (Fig. 4, *G* and *E*). It is tempting to postulate that phosphorylation of hsp27 may be a determinant factor in controlling the interaction of hsp27 with p38 kinase. To verify this, the phosphorylation of hsp27 in the cells was stably transfected with either hsp27 or its mutant hsp27-3A, and the phosphorylation of the endogenous Akt and p38 in wild-type cells was analyzed by immunoblotting after treatment of the cells with H_2O_2 or AA. As Fig. 6 shows, H_2O_2 resulted in a marked time-dependent activation of p38 but a relatively low activation of Akt (phosphorylation at Ser-473) (Fig. 6*A*), whereas AA led to a marked activation of Akt but almost no activation of p38 (Fig. 6*B*). Both H_2O_2 and AA caused phosphorylation of hsp27 (at Ser-82) in the cells stably transfected with wild-type hsp27 but not in the cells overexpressing the functionally dead hsp27 mutant (see the *second lane* on the *left* and the *far right lane* in Fig. 6, *D* and *F*). To fully demonstrate that either p38 activation or Akt activation is responsible for the phosphorylation of hsp27, either SB203580 (the selective inhibitor of p38) and siRNA for p38 mRNA or wortmannin (the selective inhibitor of PI3K) and siRNA for Akt1 mRNA were used to suppress the p38 activation and Akt activation, respectively. As expected, it was observed that suppression of p38 or Akt activation either by its selective inhibitor or by knocking its expression down with its small interference RNA blocked the H_2O_2- or AA-induced phosphorylation of hsp27 (at Ser-82), respectively (Fig. 6, *D* and *F*). Taking all the data together, our study provides solid evidence showing a causal relationship between phosphorylation of hsp27 and dissociation of hsp27 from the signaling complex.

MK2 Mediates the Interaction of p38 with hsp27—It has been generally accepted that activated p38 phosphorylates and activates downstream kinase MK2 that in turn phosphorylates hsp27 at serines 15, 78, and 82 (39). To clarify the role of MK2 in regulating the signaling complex, mouse embryo fibroblast cells from MK2 knock-out mice, MEF MK2$^{-/-}$ cells, were co-transfected with CFP-hsp27 and YFP-p38 to see if p38 kinase still interacts with hsp27 without MK2. Wild-type mouse embryo fibroblast cells, MEF MK2$^{+/+}$ cells, were used as control. The results are shown in Fig. 7. Similar to that in L929 cells, the fluorescence lifetime of the hsp27-fused CFP increased gradually from 1.65 to 1.93 ns within 30 min in MEF MK2$^{+/+}$ cells (corresponding to FRET efficiency of (18.4 ± 0.7)% to (1.8 ±

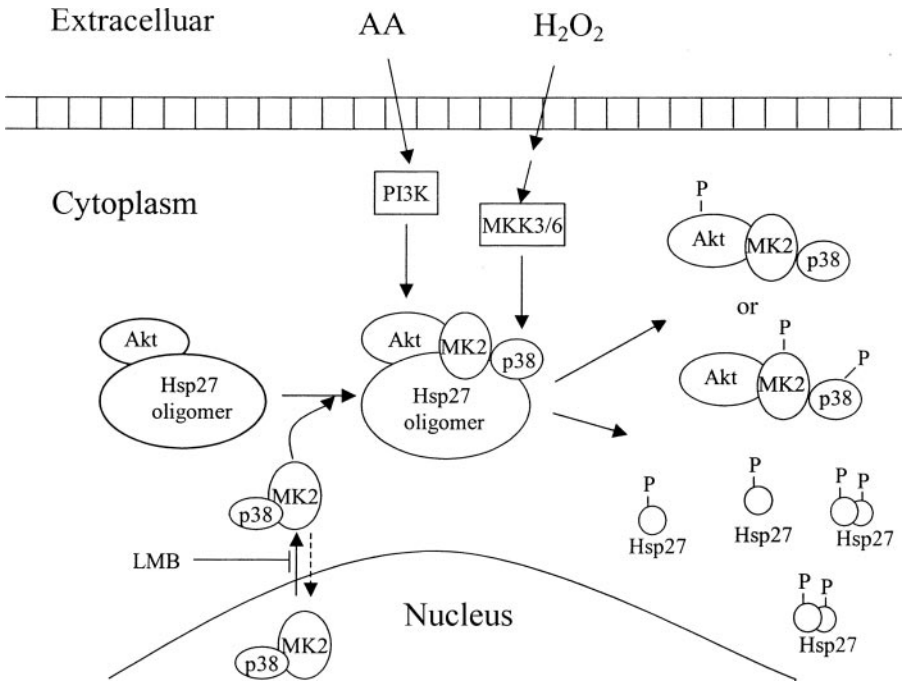

FIGURE 8. **The proposed mode for the formation and dissociation of the signaling complex containing p38 MAPK, Akt, MK2, and hsp27 in cells before and after activation of MKK3/6-p38 or PI3K/Akt signaling.**

0.4)%, respectively) after exposure to H_2O_2 (Fig. 7, *A* and *D*), indicating dissociation of hsp27 from p38 after activation of p38. However, in the co-transfected MEF MK2$^{-/-}$ cells, the fluorescence lifetime of the hsp27-fused CFP remained unchanged at a level similar to that in the absence of YFP-p38 no matter whether the cells were exposed to H_2O_2 or not (Fig. 7*B*). This indicates no interaction between hsp27 and p38 in the cells without MK2. To further examine the role of MK2 in the interaction between these two proteins, leptomycin B (LMB), which inhibits the interaction of exportin 1 with the Rev-type leucine-rich nuclear export signal (40, 41), was used to block export of MK2 from nucleus to cytosol in MEF MK2$^{+/+}$ cells (42). As shown in Fig. 7 (*C* and *D*), the interaction of p38 with hsp27 in the wild-type MEF cells co-transfected with both chimeras gradually disappeared within 20 min after addition of 5 ng/ml LMB. The corresponding fluorescence lifetime of the hsp27-fused CFP increased from 1.68 to 1.93 ns, and the FRET efficiency between the two fusion proteins decreased from 19.1 ± 1.3% to 5.9 ± 0.5% (n = 3). The results obtained with both MEF MK2$^{-/-}$ and MEF MK2$^{+/+}$ cells treated with LMB strongly suggest that p38 no longer interacts with hsp27 if cell lacks MK2 regardless of p38 activation.

To further confirm the above conclusion, analysis of the immunoprecipitate with either anti-Akt1/2 antibody or normal IgG was performed in MEF MK2$^{-/-}$ and MEF MK2$^{+/+}$ cells. As Fig. 7*E* shows, p38, hsp27, and MK2 were found in the precipitate with anti-Akt1/2 antibody from MEF MK2$^{+/+}$ cells, but only hsp27 was found in the precipitate with anti-Akt1/2 antibody from MEF MK2$^{+/+}$ cells. Almost no p38, hsp27, and MK2 could be detected in the precipitate with normal IgG in either type of cell. It was little surprise to find that hsp27 was constitutively associated with Akt whether MK2 is present or not. This observation may suggest that Akt and hsp27 form a precursory complex, and then form the signaling complex with p38 MAPK and MK2. MK2 plays a role as mediator in the complex formation.

DISCUSSION

The signal is transduced in the form of the phosphorylation event from an upstream kinase to a downstream molecule. To enable the transduction more efficient and specific, the molecules in a signaling cascade often form a complex. The signaling complex consisting of p38 kinase, MK2, Akt, and hsp27 represents a good model for studying protein-protein interaction in signal transduction and the regulation of the complex. In the present study, the interaction of p38 MAPK with hsp27 was visualized in a single living cell with the FLIM-based FRET technology. To justify the FRET approach, i.e. to test whether the fusion with fluorescent protein alters functions of p38 and hsp27, activity assay and immunoprecipitation studies were performed. These methods proved that fusion with fluorescent proteins CFP and YFP affects neither biological function of hsp27 and p38 nor prevents them from forming complexes with Akt and MK2 in the L929 and MEF MK2$^{+/+}$ cells.

These data demonstrate that hsp27 is constitutively associated with p38 in normal growing cells. However, this association does not exist in MK2-negative MEF MK2$^{-/-}$ cells or in MK2-positive MEF MK2$^{+/+}$ cells treated with LMB that blocks translocation of MK2 from nucleus to cytosol. These observations clearly indicate that the presence of MK2 is a necessary condition for the formation of p38 kinase-MK2-hsp27 signaling complex in cells. This point is further confirmed by co-immunoprecipitation analysis. It has been reported that docking interaction through a site outside the catalytic domain of MAPKs regulates the efficiency and specificity of the enzymatic reactions in the MAPK cascades (43). The docking site on p38 termed as the CD domain and a site on p38 or ERK2 MAPKs, which is termed as the ED site and regulates the docking specificity to MAPKAPKs, have been identified (44). The docking interaction of p38 with MK2 masks the nuclear localization signal sequence on MK2 and induces the translocation of MK2 to the signaling complex in cytoplasm. The finding that MK2 mediates formation of the p38-MK2-Akt-hsp27 complex may imply the importance of MK2 in p38 MAPK and PI3K/Akt signaling. As an example, MK2$^{-/-}$ neutrophils showed a partial loss of directionality, a lower protein level of p38, and a loss of *N*-formyl-methionyl-leucyl-phenylalanine-induced extracellular signal-related kinase phosphorylation in comparison with wild-type neutro-

phils (45). It was also reported that p38-dependent MK2 activation functions as 3-phosphoinositide-dependent kinase-2 to activate Akt in human neutrophils (20).

In this study, H_2O_2 and AA was used to stimulate cells to activate p38 and Akt, respectively. It was found that activation of either p38 or Akt disrupted the interaction between p38 and hsp27. Meanwhile, inhibition of p38 and Akt activation by selective inhibitors or mutation of the Thr-Gly-Tyr (TGY) dual phosphorylation motif on p38 prevented hsp27 from dissociating from p38. Because activation of either p38 or Akt leads to phosphorylation of hsp27 (21, 46), it was examined if the disruption of the interaction is attributed to phosphorylation of hsp27. For this reason, the functionally dead mutant of hsp27 (hsp27-3A), which cannot be phosphorylated (39), was fused to CFP and co-transfected with YFP-p38 into cells. It was found again that the mutant kept its interaction with p38 whether p38 or Akt was activated or not. Taking all abovementioned results together, we conclude that phosphorylation of hsp27 causes disruption of the interaction between p38 and hsp27. Non-phosphorylated hsp27 usually forms in the large homo-oligomers of the cells of up to 700 kDa, and phosphorylation is associated with a modification of its quaternary structure. Therefore, hsp27 dissociates into dimmers and monomers upon phosphorylation (47, 48). The phosphorylation-induced dissociation into dimmers and monomers is possibly the main cause for loss of the interaction between hsp27 and p38 kinase. Rane *et al.* (21) has already demonstrated that phosphorylation of hsp27 by Akt results in its dissociation from Akt both *in vitro* and *in vivo*. By directly visualizing the images of the hsp27 molecules in living cells, our study further demonstrates that hsp27 directly interacts with p38 MAPK in the signaling complex and that phosphorylation of hsp27 caused by activation of Akt or p38 results in dissociation of hsp27 from the complex.

Although a specific association of hsp27 with Akt has been reported *in vitro* in biochemical systems (21), in COS-7 cells (49), PC12 cells (22), and neutrophils (20), either the association is only connected to the complex with p38 or the association was not specified under any condition. In this study, we found that the association of hsp27 with Akt did not depend on p38 and MK2. Based on this finding and all other results obtained from FRET and immunoprecipitation studies, we may propose a model to outline the formation and dissociation of the signaling complex as shown as in Fig. 8. In unstimulated cells, inactive p38 docks with unphosphorylated MK2 in nucleus. The docking interaction masks the nuclear localization signal sequence and perhaps also unmasks a nuclear export signal sequence of MK2, which induces the translocation of MK2 and p38 together from nucleus to cytoplasm and enters the signaling complex (50). The translocation of MK2 to cytoplasm could be blocked by LMB. Upon triggering either MKK3/6-p38 or PI3K/Akt signaling, the activated p38-phosphorylated MK2 or the activated Akt leads to phosphorylation of hsp27, which results in structural change of hsp27 oligomer to monomers or dimmers and ultimate dissociation from the signaling complex.

Acknowledgments—We thank Prof. M. Gaestel (Medical School Hannover, Germany) and Prof. L. A. Weber (Dept. of Biology, University of Nevada, Reno, NV) for providing experimental materials.

REFERENCES

1. Ono, K., and Han, J. (2000) *Cell. Signal.* **12,** 1–13
2. Nebreda, A. R., and Porras, A. (2000) *Trends Biochem. Sci.* **25,** 257–260
3. Gething, M. J., and Sambrook, J. (1992) *Nature* **355,** 33–45
4. Marini, M., Frabetti, F., Musiani, D., and Franceschi, C. (1996) *Int. J. Radiat. Biol.* **70,** 337–350
5. Mehlen, P., Briolay, J., Smith, L., Diaz-Latoud, C., Fabre, N., Pauli, D., and Arrigo, A. P. (1995) *Eur. J. Biochem.* **215,** 277–284
6. New, L., and Han, J. (1998) *Trends Cardiovasc. Med.* **8,** 220–228
7. Kozawa, O., Niwa, M., Matsuno, H., Ishisaki, A., Kato, K., and Uematsu, T. (2001) *Arch. Biochem. Biophys.* **388,** 237–242
8. Ricci, J. E., Maulon, L., Battaglione-Hofman, V., Bertolotto, C., Luciano, F., Mari, B., Hofman, P., and Auberger, P. (2001) *Eur. Cytokine Netw.* **12,** 126–134
9. Jakob, U., Gaestel, M., Engel, K., and Buchner, J. (1993) *J. Biol. Chem.* **268,** 1517–1520
10. Schafer, C., Clapp, P., Welsh, M. J., Benndorf, R., and Williams, J. A. (1999) *Am. J. Physiol.* **277,** C1032–C1043
11. Nakatsue, T., Katoh, I., Nakamura, S., Takahashi, Y., Ikawa, Y., and Yoshinaka, Y. (1998) *Biochem. Biophys. Res. Commun.* **253,** 59–64
12. Pichon, S., Bryckaert, M., and Berrou, E. (2004) *J. Cell Sci.* **117,** 2569–2577
13. Marais, E., Genade, S., Salie, R., Huisamen, B., Maritz, S., Moolman, J. A., and Lochner, A. (2004) *Basic Res. Cardiol.* **100,** 35–47
14. Garrington, T. P., and Johnson, G. L. (1999) *Curr. Opin. Cell Biol.* **11,** 211–218
15. Widmann, C., Gibson, S., Jarpe, M. B., and Johnson, G. L. (1999) *Physiol. Rev.* **79,** 143–180
16. Freshney, N. W., Rawlinson, L., Guesdon, F., Jones, E., Cowley, S., Hsuan, J., and Saklatvala, J. (1994) *Cell* **78,** 1039–1049
17. Rouse, J., Cohen, P., Trigon, S., Morange, M., Alonso-Llamazares, A., Zamanillo, D., Hunt, T., and Nebreda, A. R. (1994) *Cell* **78,** 1027–1037
18. Schaeffer, H. J., Catling, A. D., Eblen, S. T., Collier, L. S., Krauss, A., and Weber, M. J. (1998) *Science* **281,** 1668–1671
19. Whitmarsh, A. J., Cavanagh, J., Tournier, C., Yasuda, J., and Davis, R. J. A. (1998) *Science* **281,** 1671–1674
20. Rane, M. J., Coxon, P. Y., Powell, D. W., Webster, R., Klein, J. B., Pierce, W., Ping, P., and McLeish, K. R. (2001) *J. Biol. Chem.* **276,** 3517–3523
21. Rane, M. J., Pan, Y., Singh, S., Powell, D. W., Wu, R., Cummins, T., Chen, Q., McLeish, K. R., and Klein, J. B. (2003) *J. Biol. Chem.* **278,** 27828–27835
22. Mearow, K. M., Dodge, M. E., Rahimtula, M., and Yegappan, C. (2002) *J. Neurochem.* **83,** 452–462
23. Nguyen, A., Chen, P., and Cai, H. (2004) *FEBS Lett.* **572,** 307–313
24. Yamboliev, I. A., Hedges, J. C., Mutnick, J. L., Adam, L. P., and Gerthoffer, W. T. (2000) *Am. J. Physiol.* **278,** H1899–H1907
25. Krump, E., Sanghera, J. S., Pelech, S. L., Furuya, W., and Grinstein, S. (1997) *J. Biol. Chem.* **272,** 937–944
26. Zu, Y. L., Qi, J., Gilchrist, A., Fernandez, G. A., Vazquez-Abad, D., Kreutzer, D. L., Huang, C. K., and Sha'afi, R. I. (1998) *J. Immunol.* **160,** 1982–1989
27. Jares-Erijman, E., and Jovin, T. (2003) *Nat. Biotechnol* **21,** 1387–1395
28. Wouters, F., Verveer, P., and Bastiaens, P. (2001) *Trends Cell Biol.* **11,** 203–211
29. Sekar, R. B., and Periasamy, A. (2003) *J. Cell Biol.* **160,** 629–633
30. Kotlyarov, A., Neininger, A., Schubert, C., Eckert, R., Birchmeier C., Volk, H. D., and Gaestel, M. (1999) *Nat. Cell Biol.* **1,** 94–97
31. Xia, Z., and Liu, Y. (2001) *Biophys. J.* **81,** 2395–2402
32. Katome, T., Obata, T., Matsushima, R., Masuyama, N., Cantley, L. C., Gotoh, Y., Kishi, K., Shiota, H., and Ebina, Y. (2003) *J. Biol. Chem.* **278,** 28312–28323
33. Cao, W., Collins, Q. F., Becker, T. C., Robidoux, J., Lupo, E. G., Jr., Xiong, Y., Daniel, K. W., Floering, L., and Collins, S. (2005) *J. Biol. Chem.* **280,**

42731–42737
34. Tong, L., Pav, S., White, D. M., Rogers, S., Crane, K. M., Cywin, C. L., Brown, M. L., and Pargellis, C. A. (1997) *Nat. Struct. Biol.* **4,** 311–316
35. Reiling, N., Blumenthal, A., Flad, H. D., Ernst, M., and Ehlers, S. (2001) *J. Immunol.* **167,** 3339–3345
36. Hii, C. S. T., Moghadammi, N., Dunbar, A., and A., F. (2001) *J. Biol. Chem.* **276,** 27246–27255
37. Yano, H., Nakanishi, S., Kimura, K., Hanai, N., Saitoh, Y., Fukui, Y., Nonomura, Y., and Matsuda, Y. (1993) *J. Biol. Chem.* **268,** 25846–25856
38. Arcaro, A., and Wymann, M. P. (1993) *Biochem. J.* **296,** 297–301
39. Stokoe, D., Engel, K., Campbell, D. G., Cohen, P., and Gaestel, M. (1992) *FEBS Lett.* **313,** 307–313
40. Fukuda, M., Asano, S., Nakamura, T., Adachi, M., Yoshida, M., Yanagida, M., and Nishida, E. (1997) *Nature* **390,** 308–311
41. Wolff, B., Sanglier, J. J., and Wang, Y. (1997) *Chem. Biol.* **4,** 139–147
42. Engel, K., Kotlyarov, A., and Gaestel, M. (1998) *EMBO J.* **17,** 3363–3371
43. Tanoue, T., and Nishida, E. (2002) *Pharmacol. Ther.* **93,** 193–202
44. Tanoue, T., Maeda, R., Adachi, M., and Nishida, E. (2001) *EMBO J.* **20,** 466–479
45. Hannigan, M. O., Zhan, L., Ai, Y., Kotlyarov, A., Gaestel, M., and Huang, C.-K. (2001) *J. Immunol.* **167,** 3953–3961
46. Tanabe, K., Akamatsu, S., Suga, H., Takai, S., Kato, K., Dohi, S., and Kozawa, O. (2005) *J. Cell. Biochem.* **96,** 56–64
47. Lambert, H., Charette, S. J., Bernier, A. F., Guimond, A., and Landry, J. (1999) *J. Biol. Chem.* 9378–9385
48. Rogalla, T., Ehrnsperger, M., Preville, X., Kotlyarov, A., Lutsch, G., Ducasse, C., Paul, C., Wieske, M., Arrigo, A.-P., Buchner, J., and Gaestel, M. (1999) *J. Biol. Chem.* **274,** 18947–18956
49. Konishi, H., Matsuzaki, H., Tanaka, M., Takemura, Y., Kuroda, S., Ono, Y., and Kikkawa, U. (1997) *FEBS Lett.* **410,** 493–4988
50. Ben-Levy, R., Hooper, S., Wilson, R., Paterson, H. F., and Marshall, C. J. (1998) *Curr. Biol.* **8,** 1049–1057